Available online at www.sciencedirect.com
ScienceDirect
Polymer 47 (2006) 7391–7396
polymer
www.elsevier.com/locate/polymer

# Cylindrical polyelectrolyte-comb-surfactant complexes

Sabrina Duschner [a], Franziska Gröhn [b], Michael Maskos [a,*]

[a] Institut für Physikalische Chemie, Universität Mainz, Welder Weg 11, D-55099 Mainz, Germany
[b] Max-Planck-Institut für Polymerforschung, Ackermannweg 10, D-55128 Mainz, Germany

Received 7 April 2006; received in revised form 22 August 2006; accepted 23 August 2006
Available online 12 September 2006

**Abstract**

Quaternized polymer combs based on poly(2-vinylpyridine-macromonomers) and the surfactant sodium dodecylsulfate are employed in the synthesis of a novel cylindrical polyelectrolyte-comb-surfactant complex (PECSC). The complex formed has 1:1 stoichiometry with respect to the ratio of dodecylsulfate to pyridinium units. It is soluble in organic solvents such as 2-butanol or chloroform. Characterization of single particle properties of the complex in organic solution is possible and yields a radius of gyration of $\langle R_g \rangle_z = 78.4$ nm, a hydrodynamic radius of $\langle 1/R_h \rangle_z^{-1} = 51.4$ nm and a cross-sectional radius of $R_{g,cross} = 3.9$ nm in chloroform. The characteristic ratio $\gamma = \langle R_g \rangle_z / \langle 1/R_h \rangle_z^{-1}$ decreases from $\gamma = 1.73$ for the original quaternized polymer comb, indicating the semi-flexible, cylindrical nature of the macromolecules in aqueous solution, to $\gamma = 1.53$ for the complex in chloroform. The effect of the main-chain stretching accompanied by the increase of the volume of the comb by introduction of the surfactant is smaller as compared to the electrostatic interactions in the parent comb. This is also reflected in the persistence length $l_p$, which is determined by SANS, and found to be 21.3 nm for the complex and 24.4 nm for the polyelectrolyte comb. In addition, AFM investigations of the polymers adsorbed onto mica showed a 2D-equilibrium adsorption for the complex and a kinetically dominated adsorption process in case of the polyelectrolyte comb.


*Keywords:* Macromonomers; Comb-Polymer; Polyelectrolyte-surfactant-complex

## 1. Introduction

Polyelectrolyte–surfactant complexes are complexes between linear polyelectrolytes and surfactants that spontaneously form and precipitate from aqueous solution [1]. The main driving forces for the complex formation are the counter-ion exchange and the hydrophobic interaction of the surfactant, which typically leads to a 1:1 complex formation between the charges of the polyelectrolyte and the oppositely charged surfactant. Their solid state properties include good film-forming behavior and complex mesophase-separated morphologies [2–17].

In the present study, the complexation of cylindrically shaped polyelectrolytes and oppositely charged surfactants is employed to synthesize cylindrically shaped polyelectrolyte-comb-surfactant complexes (PECSC). Polymer combs with high grafting density such as polymacromonomers have to adopt a cylindrical shape mainly due to the sterical hindrance induced by the oligomeric side chains, which prevents the otherwise coil-like main chain from coiling [18–21]. Bulk properties include liquid crystalline bulk properties [22]. Unfortunately, most of the described systems have rather poor film-forming properties. In order to combine the versatile film-forming properties known from many polyelectrolyte–surfactant complexes with the cylindrical macromolecular shape of the polymer combs, polyelectrolyte-comb polymers are complexed with surfactants. As polymer comb we employ poly(2-vinylpyridine-macromonomers) that are quaternized with ethylbromide. Complexation of the polyelectrolyte comb is accomplished by the addition of sodium dodecylsulfate in aqueous solution. The resulting PECSC is isolated and subsequently characterized in solution by static and dynamic light scattering (SLS, DLS), small-angle neutron scattering (SANS) and atomic force microscopy (AFM) after spin casting from organic solution.

* Corresponding author.
*E-mail addresses:* duschnes@uni-mainz.de (S. Duschner), groehn@mpip-mainz.mpg.de (F. Gröhn), maskos@uni-mainz.de (M. Maskos).

0032-3861/$ - see front matter © 2006 Elsevier Ltd. All rights reserved.
doi:10.1016/j.polymer.2006.08.060

## 2. Experimental section

### 2.1. Instrumentation

Static and dynamic light scattering experiments were performed at 20 °C using an ALV-SP-86 goniometer, an ALV-3000 correlator, an 25 mW Uniphase HeNe laser $\lambda_0 = 632.8$ nm and an ALV/High QEAPD avalanche diode fiberoptic detection system. Measurements were carried out from 30° to 150° in angular steps of 5°. The refractive index measurements were performed with an in-house built interferometric instrument [23]. AFM-micrographs were recorded in tapping mode, using a Nanoscope IIIa multi-mode instrument (Digital Instruments). Small-angle neutron scattering (SANS) was performed at D11 beamline, Institute Laue-Langevin (ILL), Grenoble, France, at a wavelength of 0.6 nm, a wavelength spread of 11% and at scattering vectors between 0.032 and 3.0 $nm^{-1}$. Data treatment included standard procedures for background subtraction, radial averaging and absolute calibration.

### 2.2. Materials

Sodium dodecylsulfate (Fluka), tetrabutylammonium bromide (Fluka), chloroform (>99.8%, Fisher Scientific), 2-butanol (>99.5%, Fluka) were used as received. Water was purified with a Milli-Q deionizing system (Waters) before use.

### 2.3. Sample preparation

Solutions for light scattering experiments were filtered before measurement using Millex-LG filters (0.20 μm pore size, hydrophilic PTFE). Samples for atomic force microscopy were prepared by spin casting from solution on freshly cleaved mica (polymer concentrations in the range of 10–30 mg/L).

### 2.4. Synthesis

The poly(2-vinylpyridine)-brush was synthesized via a free radical polymerization of poly(2-vinylpyridine) macromonomers with a methacrylate end group as described elsewhere [20]. The number average of the molar mass of the macromonomer was determined by MALDI-TOF $M_n =$ 2850 g/mol and the polydispersity $M_w/M_n = 1.06$. The weight average of the molecular weight of the poly(2-vinylpyridine)-brush was determined $M_w = 5.4 \times 10^6$ g/mol by static light scattering in DMF containing $1.15 \times 10^{-2}$ mol/L LiBr [24]. The quaternization reaction was carried out in nitromethane at 60° C for one week under an argon atmosphere using 1 g of the poly(2-vinylpyridine)-brush (35 mmol PVP side chains) and a tenfold molar excess of ethylbromide [25,26]. The polyelectrolyte was characterized using elemental analysis yielding a degree of quaternization of 50 mol%, which corresponds to a number average of the molar mass per side chain of $M_n = 4270$ g/mol. Quaternized poly(2-vinylpyridine)-comb (0.059 mmol, 250 mg, quaternized PVP side chains) were dissolved in 250 mL of water. To the stirred polymer solution a concentrated solution (200 mg/mL) of sodium dodecylsulfate was added dropwise. After addition of 1.1 mL (0.764 mmol) the formation of a white precipitate was observed. The product was isolated and subsequently purified by ultrafiltration in water to remove any residual surfactant using a regenerated cellulose ultrafiltration membrane (Millipore Ultracel PLGC, 10 kDa NMWL, 76 mm filter diameter). A conversion of 100 mol% with respect to quaternized PVP was proven by elemental analysis and no significant residual bromide was found (<0.2 wt%). Using the results from elemental analysis, the number average of the molar mass per side chain of the complex was calculated, $M_n = 6670$ g/mol.

## 3. Results and discussion

The quaternized polymer comb containing poly(2-vinylethylpyridinium bromide)-sidechains was synthesized by quaternization of the corresponding poly(2-vinylpyridine)-based polymer comb [24,25]. The degree of quaternization of 50 mol% was determined by elemental analysis. The data obtained by characterization in solution are summarized in Table 1.

As indicated in Fig. 1, addition of an aqueous solution of sodium dodecylsulfate to the aqueous solution of the quaternized polymer comb leads to the spontaneous formation of the complex (PECSC), which precipitates from solution. The complex formation is basically comparable to the procedure

Table 1
Characterization of the polymers

| Sample | $M_{w,app}$ (g/mol)[a] | $M_{w,calc}$ (g/mol) | $A_2$ (mL mol/$g^2$)[a] | d$n$/d$c$, solvent | d$n$/d$c$, calculated | $\langle R_g \rangle_{z,app}$ (nm) | $\langle 1/R_h \rangle^{-1}_{z,app}$ (nm) | $\gamma$[e] |
|---|---|---|---|---|---|---|---|---|
| PMM(2-VP), polymacromonomer | $5.4 \times 10^6$ | | $1.4 \times 10^{-5}$ | 0.153 mL/g, DMF, $1.15 \times 10^{-2}$ mol/L LiBr | | 68.4 | 45.2 | 1.51 |
| QPMM(2-VEtP-Br), quaternized PMM | $7.3 \times 10^6$ | $8.1 \times 10^6$[b] | $1.0 \times 10^{-5}$ | 0.183 mL/g, water, $5 \times 10^{-3}$ mol/L NaBr | 0.173 mL/g[d] | 88.2 | 51.0 | 1.73 |
| QPMM(2-VEtP-SDS), PECSC complex | $14.3 \times 10^6$ | $12.7 \times 10^6$[c] | $1.8 \times 10^{-5}$ | 0.081 mL/g, $CHCl_3$, $10^{-4}$ mol/L ($n$-butyl)$_4$NBr | 0.086 mL/g[d] | 78.4 | 51.4 | 1.53 |

[a] Static light scattering.
[b] Calculated from PMM(2-VP) with 50% degree of quaternization.
[c] Calculated from footnote b with 100% complex formation.
[d] Calculated from footnote b or c, respectively.
[e] Characteristic ratio $\gamma = \langle R_g \rangle_{z,app} / \langle 1/R_h \rangle^{-1}_{z,app}$.

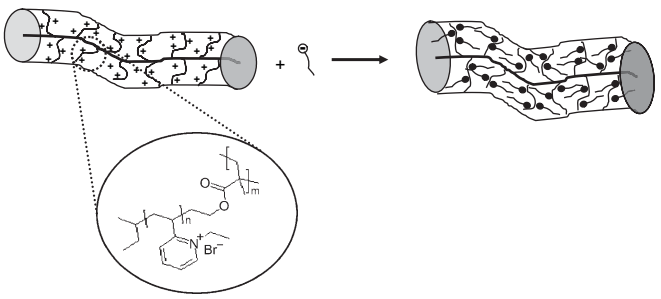

Fig. 1. Schematic picture of the complexation of the polyelectrolyte comb polymer and the surfactant leading to the formation of semi-flexible, cylindrical complexes.

already described for linear polyelectrolytes and their complexation with oppositely charged surfactants and is driven by the counter-ion exchange and the hydrophobic interaction of the surfactant [1,2]. After isolation and purification, the complex is redispersed in organic solvents such as 2-butanol or chloroform.

A solution of the complex in chloroform shows small residual influence of polyelectrolyte-like behavior, which can be seen by a curvature in the $q$-dependence of the SLS-data (data not shown). In order to determine single particle properties, $5 \times 10^{-5}$ mol/L tetrabutylammonium bromide was added to the solution, which successfully suppresses the undesired effects and a Zimm-plot as shown in Fig. 2 is obtained.

From this, the weight average molecular weight $M_w$, the $z$-average of the radius of gyration $\langle R_g \rangle_{z,app}$ and the second virial coefficient $A_2$ are obtained. The determined molecular weight increase is in accordance with the expected value (see Table 1) and corresponds to a 1:1 complex formation between the dodecylsulfate and the pyridinium groups. The deviations of less than 10% are attributed to the error in the determination of d$n$/d$c$, which for example has not been measured in the Donnan equilibrium [27]. In addition, elemental analysis confirms the result of complete counter-ion exchange.

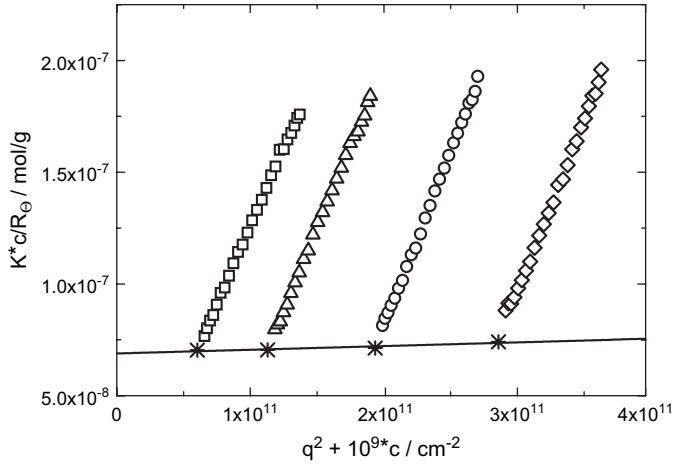


Fig. 2. Zimm-plot of the complex QPMM(2-VEtP-SDS) in chloroform, $5 \times 10^{-5}$ mol/L $n$-tetrabutylammonium bromide (square: $c = 0.060$ g/L; triangle: $c = 0.113$ g/L; circle: $c = 0.194$ g/L; rhomb: $c = 0.286$ g/L).

Both, the radius of gyration $\langle R_g \rangle_{z,app}$ and the hydrodynamic radius $\langle 1/R_h \rangle^{-1}_{z,app}$, as obtained by DLS, increase as compared to the parent poly(2-vinylpyridine)-polymer comb.

The solvent quality as indicated by the $A_2$-values is comparable for each of the samples (Table 1). As seen in Table 1, the characteristic ratio, which is a measure for the shape of the molecules and indicates in all characterized samples their semi-flexible, cylindrical character, increases from $\gamma = 1.51$ to $\gamma = 1.73$ after the quaternization reaction. This is attributed to the electrostatic repulsion in the quaternized polymer comb, which adds to the stretching of the main chain. Interestingly, this effect is almost reversed upon complexation ($\gamma = 1.53$). The charges are nearly fully shielded and the effect of the additionally incorporated surfactant and the accompanied increase in volume is of minor importance for the stretching of the main chain.

This is also observed by SANS (Fig. 3). First, the semi-flexible, cylindrical shape in solution is already indicated by a slope of $d_f = -1$ for an infinitely thin cylinder in a log–log plot of the scattering intensity against the value of the scattering vector $q$ at low $q$ values [28]. For the polyelectrolyte comb, this yields $d_f = -1.2$, and for the complex $d_f = -1.5$. Both values deviate from $d_f = -1$ due to the fact that the cylinders possess a finite cross-sectional radius influencing the scattering behavior in the corresponding $q$ regime. In order to remove the cross-sectional influence, the cross-sectional radius of gyration $R_{g,cross}$ is determined by the slope of a Guinier-plot ($\ln[qI(q)]$ vs. $q^2$) [28], as shown in the inset of Fig. 3a. The determination of the cross-sectional radius yields $R_{g,cross} = 3.9$ nm $\pm$ 0.5 nm for the complex and 3.1 nm $\pm$ 0.5 nm for the polyelectrolyte comb.

Fig. 3 also contains the cross-sectional radial pair-distance distribution function $P(r)$, determined from the SANS measurements by indirect Fourier-Transformation under regularization and the resulting density distribution $\rho(r)$ [28,29]. In both cases, the increase of the diameter of the complex (PECSC) compared to the polyelectrolyte comb is seen. In addition, $\rho(r)$ of the complex suggests a comparable distribution of the surfactant as compared to the distribution of the charges of the polyelectrolyte comb.

According to Holtzer, a plot of $qI(q)$ vs. $q$ shows a plateau for infinitely thin cylinders, indicating the slope of $d_f = -1$ already discussed above for the scattering behavior of thin cylinders [30]. The Holtzer-analysis of the complex after correction of the scattering attributed to the cross-section as discussed above is presented in Fig. 3d. The observed plateau clearly indicates the cylindrical nature of the complex. From this, the length per monomer is determined according to $l_{MM} = M_{MM}(\pi/A)$, where $M_{MM}$ is the molecular weight of the side chain and $A$ is the determined value of the plateau [30]. This yields $l_{MM} = 0.23$ nm for the complex, which is in reasonable good agreement with the theoretical value of $l_{MM,theo} = 0.25$ nm for a carbon-main-chain. In addition to the data analysis discussed for the complex, a fit according to the Pedersen–Schurtenberger worm-like chain model to the combined light scattering- and SANS-data yields a $R_{g,cross} = 3.7$ nm $\pm$ 0.5 nm and an apparent Kuhn length of

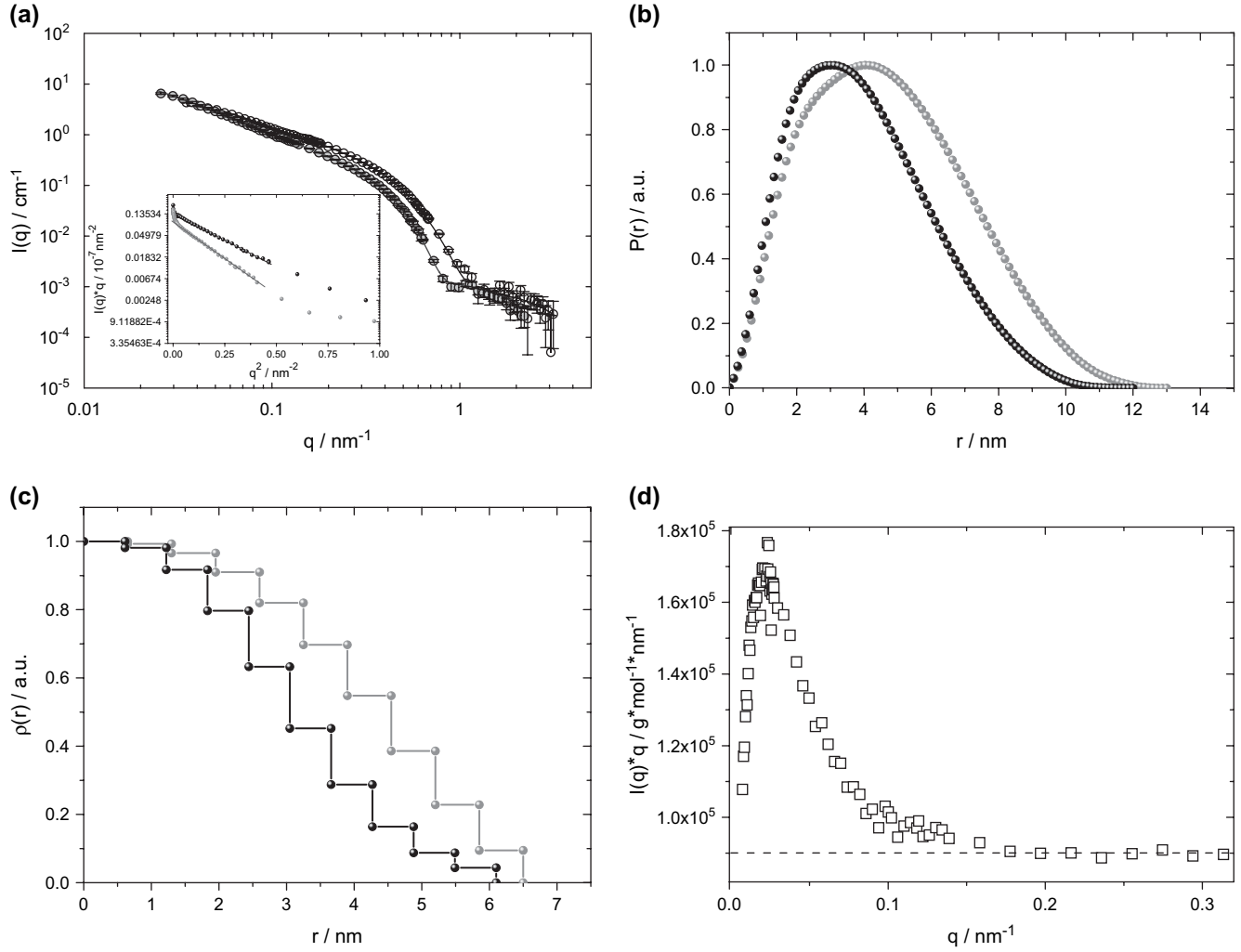


Fig. 3. (a) SANS of the polyelectrolyte comb QPMM(2-VEtP-Br) in $D_2O$, $c = 1.7$ g/L (white circles) and of the complex QPMM(2-VEtP-SDS) in $CDCl_3$, $c = 2.0$ g/L (grey circles), inset: $qI(q)$ vs. $q^2$ and linear extrapolation for the determination of $R_{g,cross}$ (QPMM(2-VEtP-Br): black, QPMM(2-VEtP-SDS): grey); (b) cross-sectional radial pair-distribution function $P(r)$ obtained from (a) (QPMM(2-VEtP-Br): black, QPMM(2-VEtP-SDS): grey); (c) density distribution $\rho(r)$ obtained from (b) (QPMM(2-VEtP-Br): black, QPMM(2-VEtP-SDS): grey); (d) Holtzer-plot of the SANS-data of the complex after correction for the cross-section, dashed line: plateau.

$l_{k,app} = 42.6$ nm $\pm$ 0.5 nm, also indicating the semi-flexible nature of the cylindrical complex [31,32]. Unfortunately, extrapolation to zero concentration has not been possible due to the already low count rates at the employed rather dilute concentration. Also, polydispersity was not taken into account in the model. Nevertheless, an extrapolation to zero concentration as well as polydispersity is not likely to influence the Kuhn length and the cross-sectional radius of gyration, as recently shown by Zhang et al. [33]. For the polyelectrolyte comb, the corresponding analysis of the SANS-data yields $R_{g,cross} = 3.2$ nm $\pm$ 0.5 nm and an apparent Kuhn length of $l_{k,app} = 48.8$ nm $\pm$ 1.0 nm, which also are in good agreement with the Guinier-analysis. All results obtained from experiments in dilute solution can be attributed to single particle properties.

The structure of the complex as compared to the polyelectrolyte comb was also investigated on a solid substrate by AFM. Fig. 4 shows an AFM picture obtained after spin casting from chloroform onto mica.

The same picture also shows an AFM of the parent quaternized polyelectrolyte combs. The electrostatic interactions between the positively charged polyelectrolyte and the negatively charged mica surface lead to intense adsorption of the polyelectrolyte combs, which appear bended and coiled. In contrast, the complex does not show this behavior.

Quantitative analysis of the AFM pictures allows the determination of the average values of the two dimensional squared end-to-end radius $\langle R^2 \rangle$ and the contour length $\langle l_c \rangle$. A different relation between $R^2$, $l_c$ and the persistence length $l_p$ is obtained for a worm-like chain depending on the process of adsorption onto the surface, as shown by Rivetti et al., who analyzed the structure of DNA deposited onto mica [34]. A true equilibrium adsorption results in

$$\langle R^2 \rangle_{2D} = 4 l_p l_c \left( 1 - \frac{2 l_p}{l_c} \left( 1 - \exp\left[ -\frac{l_c}{2 l_p} \right] \right) \right),$$

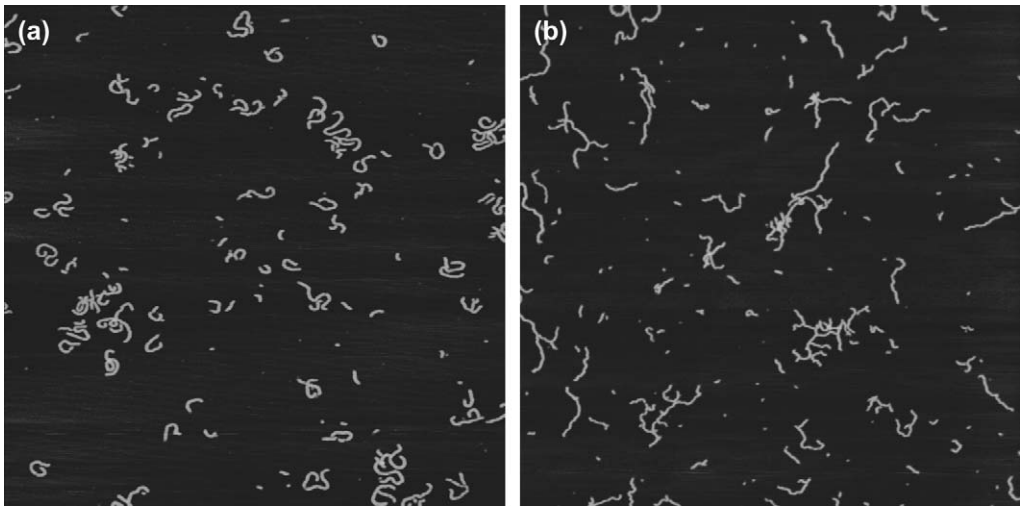


Fig. 4. (a) AFM (height) of the polyelectrolyte comb QPMM(2-VEtP-Br), spincast from water ($c = 10$ mg/L) onto mica (size: 2 μm × 2 μm); (b) AFM (height) of the complex QPMM(2-VEtP-SDS), spincast from chloroform ($c = 10$ mg/L) onto mica (size: 2 μm × 2 μm).

whereas an adsorption controlled by kinetic trapping can be described by a three-to-two dimensional projection:

$$\langle R^2 \rangle_{3D\to 2D} = \frac{1}{3}\langle R^2 \rangle_{2D}.$$

The statistical analysis of 708 molecules yields for the complex $(\langle R^2\rangle)^{0.5} = 89.0\ \text{nm} \pm 28\%$ and $\langle l_c\rangle = 130\ \text{nm} \pm 32\%$. From these values, the persistence length $l_p$ can be determined according to the models described above and the results are shown in Fig. 5.

In case of the three-to-two dimensional projection, the determined $(\langle R^2\rangle)^{0.5}$ can never be reached with any $l_p$ (data not shown). In contrast, $l_p = 22.7$ nm is obtained for the

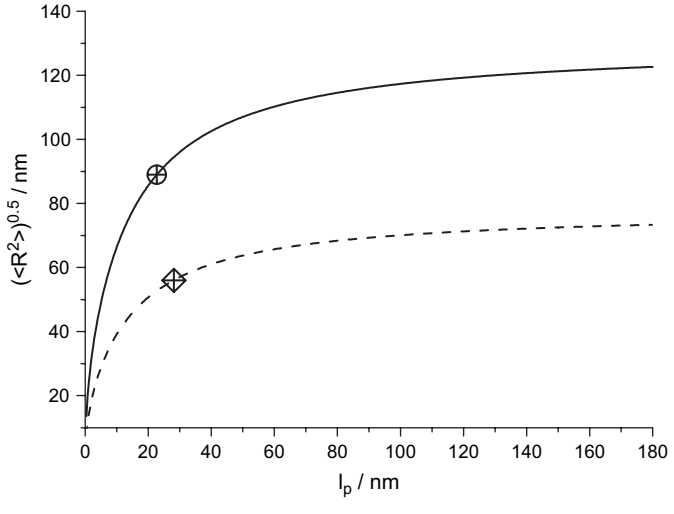


Fig. 5. $(\langle R^2\rangle)^{0.5}$ vs. $l_p$ according to the models described in the text. Solid line: PECS complex, 2D equilibrium adsorption with $\langle l_c\rangle = 130$ nm (crossed circle indicates the value of $l_p = 22.7$ nm for the experimentally determined $(\langle R^2\rangle)^{0.5} = 89.0$ nm); dashed line: polyelectrolyte comb QPMM(2-VEtP-Br), three-to-two dimensional projection with $\langle l_c\rangle = 135$ nm (crossed rhomb indicates the value of $l_p = 28.1$ nm for the experimentally determined $(\langle R^2\rangle)^{0.5} = 56.0$ nm).

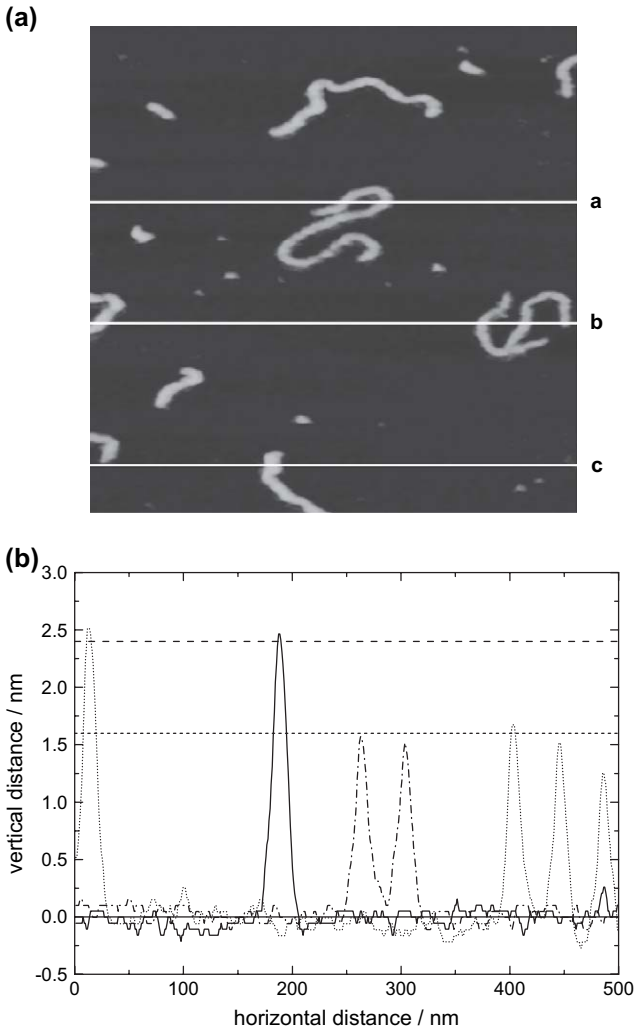


Fig. 6. (a) AFM (height) of the polyelectrolyte comb QPMM(2-VEtP-Br) and the complex QPMM(2-VEtP-SDS), spincast subsequently onto mica ($c = 5$ mg/L each; size: 500 nm × 500 nm; a–c: line scans); (b) line scans from Fig. 6a; (a) dash-dotted; (b) dotted; (c) solid; the lines at 1.6 nm and 2.4 nm are guides for the eye to indicate the height of the two samples.

equilibrium adsorption model. The relation between the persistence length and the Kuhn length for the worm-like chain model, $l_p = 0.5 \times l_k$, can be used to compare the results obtained by AFM and SANS. From SANS it follows $l_p = 21.3$ nm supporting the results obtained from AFM.

For the quaternized polymer comb adsorbed onto mica and studied by AFM, the statistical analysis of 361 molecules yields $(\langle R^2 \rangle)^{0.5} = 56.0\ \text{nm} \pm 26\%$ and $\langle l_c \rangle = 135\ \text{nm} \pm 44\%$. In case of the model based on the equilibrium adsorption, this would lead to $l_p = 6.4$ nm (data not shown), whereas the three-to-two dimensional projection yields $l_p = 28.1$ nm (SANS: $l_p = 24.4$ nm), thus supporting the hypothesis of kinetically controlled adsorption.

The difference between the quaternized polymer comb and the complex is also visualized in a single AFM experiment. Both samples were spin cast subsequently onto the same substrate (Fig. 6). The same results are obtained if the polyelectrolyte comb in water is deposited first onto the substrate or if the complex is applied first.

The different polymer combs are readily identified in the height profile. The complex possesses a larger height as compared to the quaternized polymer comb which can be attributed to the increase in volume and is consistent with the results obtained by SANS for $R_{g,cross}$.

## 4. Conclusions

It has been possible to synthesize a cylindrical PECSC-1:1-complex of a quaternized polymer comb and an oppositely charged surfactant. The single particle properties are determined both in solution and on a solid substrate. The semi-flexible nature of the complex in solution was characterized by SANS and light scattering. This yields a cross-sectional radius of gyration $R_{g,cross} = 3.9$ nm and a persistence length $l_p = 21.3$ nm in chloroform. A corresponding value is obtained by AFM, when the complex is adsorbed onto mica assuming a 2D equilibrium model for the adsorption. In addition, the complex shows an increased height as compared to the polyelectrolyte-comb. This also indicates the increase in diameter also observed by the scattering experiments in solution. Currently, the film-forming properties and the bulk state properties of this promising new self-assembled material are investigated.

## Acknowledgements

We would like to thank Prof. Dr. M. Schmidt and Dr. K. Fischer for helpful discussions, Dr. T. Stephan for the help in the synthesis of the polyelectrolyte and Prof. Dr. J.S. Pedersen for the help in the fit of the SANS-data. We thank Dr. R. Schweins and Dr. P. Lindner, ILL, Grenoble, for support with the SANS experiments at beamline D11.

## References

[1] Goddard ED. Colloids Surf 1986;19:301.
[2] Thünemann AF. Prog Polym Sci 2002;27:1473.
[3] Antonietti M, Conrad J, Thünemann A. Macromolecules 1994;27:6007.
[4] Ruokolainen J, ten Brinke G, Ikkala O, Torkkeli M, Serimaa R. Macromolecules 1996;29:3409.
[5] Faul CFJ, Antonietti A. Adv Mater 2003;15:673.
[6] Leonard MJ, Strey HH. Macromolecules 2003;36:9549.
[7] Nakamura K, Shikata T. Macromolecules 2003;36:9698.
[8] Bakeev KN, Shu YM, MacKnight WJ, Zezin AB, Kabanov VA. Macromolecules 1994;27:300.
[9] Antonietti M, Förster S, Zisenis M, Conrad J. Macromolecules 1995;28:2270.
[10] Bakeev KN, Shu YM, Zezin AB, Kabanov VA, Lezov AV, Mel'nikov AB, et al. Macromolecules 1996;29:1320.
[11] Ray B, El Hasri S, Guenet JM. Eur Phys J E 2003;11:315.
[12] Claesson PM, Bergström M, Dedinaite A, Kjellin M, Legrand JF, Grillo I. J Phys Chem B 2000;104:11689.
[13] Bergström LM, Kjellin URM, Claesson PM, Grillo I. J Phys Chem B 2004;108:1874.
[14] Wesley RD, Cosgrove T, Thompson L, Armes SP, Baines FL. Langmuir 2002;18:5704.
[15] Harada A, Kataoka K. Macromolecules 1995;28:5294.
[16] Holappa S, Andersson T, Kantonen L, Platter P, Tenhu H. Polymer 2003;44:7907.
[17] Berret JF, Vigolo B, Eg R, Herve P, Grillo I, Yang L. Macromolecules 2004;37:4922.
[18] Wintermantel M, Schmidt M, Tsukahara Y, Kajiwara K, Kohjiya S. Macromol Rapid Commun 1994;15:279.
[19] Wintermantel M, Gerle M, Fischer K, Schmidt M, Wataoka I, Urakawa H, et al. Macromolecules 1996;29:978.
[20] Dziezok P, Sheiko SS, Fischer K, Schmidt M, Möller M. Angew Chem Int Ed Engl 1997;36:2812.
[21] Gerle M, Fischer K, Roos S, Müller AHE, Schmidt M, Sheiko SS, et al. Macromolecules 1999;32:2629.
[22] Wintermantel M, Fischer K, Gerle M, Ries R, Schmidt M, Kajiwara K, et al. Angew Chem Int Ed Engl 1995;34:1472.
[23] Becker A, Köhler W, Müller B. Ber Bunsen Ges Phys Chem 1995;99:600.
[24] Stephan T. PhD thesis. Mainz, Germany; 2002.
[25] Stephan T, Muth S, Schmidt M. Macromolecules 2002;35:9857.
[26] Dziezok P. PhD thesis. Mainz, Germany; 1999.
[27] Vrij A, Overbeek JT. J Colloid Interface Sci 1962;17:570.
[28] Feigin LA, Svergun DI. Structure analysis by small-angle X-ray and neutron scattering. New York: Plenum Press; 1987.
[29] Glatter O. J Appl Crystallogr 1980;13:7 and 415.
[30] Holtzer A. J Polym Sci 1955;17:432.
[31] Pedersen JS, Schurtenberger P. Macromolecules 1996;29:7602.
[32] Pedersen JS, Laso M, Schurtenberger P. Phys Rev E 1996;54:R5917.
[33] Zhang B, Gröhn F, Pedersen JS, Fischer K, Schmidt M. Macromolecules, submitted for publication.
[34] Rivetti C, Guthold M, Bustamante C. J Mol Biol 1996;264:919.